A Second-Order Closure Model for the Effect of Averaging Time on Turbulent Plume Dispersion

R. I. SYKES AND R. S. GABRUK

ARAP Group, Titan Research and Technology, Princeton, New Jersey

(Manuscript received 24 April 1996, in final form 7 August 1996)

ABSTRACT

A practical model for the effect of averaging time on the turbulent dispersion of a continuous plume is presented. The model is based on a second-order turbulence closure scheme, but is applied to the integrated spatial moments of the plume to provide a Gaussian spread prediction. Velocity fluctuation variances are used directly by the closure model to predict the dispersion, and are partitioned into meandering and diffusive scales based on the instantaneous spread of the plume. Finite time averaging is represented by a simple estimate of the turbulent energy spectrum. The model is compared with short-duration atmospheric measurements for dispersing clouds.

1. Introduction

Turbulent dispersion in the atmosphere is a result of chaotic advection by a wide spectrum of eddy motions. In general, the larger-scale motions behave like a time-dependent, spatially inhomogeneous mean wind and produce coherent meandering of a pollutant cloud or plume, while the smaller-scale motions act to diffuse the pollutant and mix it with the ambient air. The distinction between the two types of motion is dependent on both the sampling procedure and the scale of the pollutant cloud.

For the case of a continuous plume of material, the duration of the sampling time (the time average period) determines the effective size of the plume. A longer time average will sample longer timescales of the meandering process and will therefore produce a wider plume. This effect has been recognized in connection with atmospheric observations, and some dispersion models have incorporated empirical adjustments based on the power-law relation of Slade (1968) to account for the averaging period. The phenomenon is particularly important for highly toxic or flammable materials, for which exposures of a relatively short duration must be considered.

As the sampling time is reduced, we approach an instantaneous snapshot of the plume, where the spread is related to the relative dispersion of two particles. The subject of instantaneous or relative dispersion, as introduced by Batchelor (1950) and Brier (1950), has been studied for many years. A designation of ''relative'' dispersion arises from consideration of the evolving separation of a pair of particles in a turbulent flow; that is, we consider the dispersion relative to the centroid of the pair rather than in a fixed Eulerian frame. This frame clearly avoids the meandering component of the turbulence since both particles will move together under the influence of a large-scale eddy, so the average relative dispersion measures the effective instantaneous separation of a cloud of particles.

The effects of time averaging have been recognized in a number of previous model studies. The instantaneous or relative dispersion models of Smith and Hay (1961) and Georgopoulos and Seinfeld (1988) are based on spectral filtering of the turbulence spectrum. A related treatment of time averaging effects is described by Eckmann (1994) using a two-particle random-walk model, where the energy available for the random walk is determined by a spectral filter technique. The detailed representation of the energy spectrum in these models demands a significant computational effort, and our objective here is the development of a simplified practical scheme for representing the effect of time averaging on plume width. The model must describe relative dispersion in the limit of short-term averages and give the absolute, or ensemble, dispersion rate for long-term sampling. We shall generalize the second-order closure ensemble dispersion model of Sykes et al. (1986) to include the effect of time averaging, so we first briefly review the basic model.

2. Ensemble dispersion model

Sykes et al. (1986) have shown that the second-order closure equations for passive plume dispersion can be

Corresponding author address: Dr. R. I. Sykes, ARAP Group, Titan Research and Technology, 50 Washington Road, P.O. Box 2229, Princeton, NJ 08543-2229.

integrated in the plane transverse to the transport direction to yield

$$\frac{d}{dt}\langle cy^2\rangle = 2\langle y\overline{v'c'}\rangle \tag{1a}$$

and

$$\frac{d}{dt}\langle cz^2\rangle = 2\langle z\overline{w'c'}\rangle, \tag{1b}$$

where y and z are lateral and vertical coordinate displacements about the plume centroid, and v and w are lateral and vertical velocity components. The angle brackets denote integration in the transverse—that is (y, z)—plane, the overbar denotes the ensemble average, and the prime denotes a turbulent fluctuation from the average. A time derivative has been used to denote the plume evolution, but this can be interpreted as spatial development, with t replaced by x/U, for a steady-state plume in a mean wind U. The plume concentration is c, and the terms on the left-hand side are identifiable as the spatial moments of the plume—that is, $\langle c\rangle\sigma_y^2$ and $\langle c\rangle\sigma_z^2$. The second-order correlations on the right-hand sides of the above equations are simply the turbulent fluxes of c in the two coordinate directions, and the objective of second-order closure theory has been the development of predictive equations for these correlations based on the conservation laws of motion. Exact equations can be written for the correlations, but these equations involve higher-order terms from the nonlinear advective terms in the conservation laws. Second-order closure, as the name implies, develops predictive equations for second-order correlations using empirical models for third-order correlations where necessary.

Using the closure model of Lewellen (1977), the equations for the flux terms can be written as

$$\frac{d}{dt}\langle y\overline{v'c'}\rangle = \langle c\rangle\overline{v'^2} - A\frac{q}{\Lambda}\langle y\overline{v'c'}\rangle \tag{2a}$$

and

$$\frac{d}{dt}\langle z\overline{w'c'}\rangle = \langle c\rangle\overline{w'^2} - A\frac{q}{\Lambda}\langle z\overline{w'c'}\rangle + \frac{g}{T_0}\langle z\overline{c'\theta'}\rangle, \tag{2b}$$

where $q^2 = \overline{u'^2} + \overline{v'^2} + \overline{w'^2}$, Λ is the turbulence length scale, and A is an empirical model constant with a value of 0.75. The vertical dispersion equations contain a gravitational buoyancy term, depending on the temperature correlation, where θ' is the temperature fluctuation, g is gravitational acceleration, and T_0 is the reference temperature for the Boussinesq approximation. The correlation term $\langle z\overline{c'\theta'}\rangle$ requires a further evolution equation, which is written using the model and notation of Lewellen (1977) as

$$\frac{d}{dt}\langle z\overline{c'\theta'}\rangle = \langle c\rangle\overline{w'\theta'} - 2bs\frac{q}{\Lambda}\langle z\overline{c'\theta'}\rangle - \frac{\partial\bar{\theta}}{\partial z}\langle z\overline{w'c'}\rangle, \tag{3}$$

where the additional model constants b and s take the values 0.125 and 1.8, respectively.

If we use the fact that the integrated plume mass $\langle c\rangle$ is conserved, then we can write the fluctuation correlation equations in terms of more familiar variables. Defining

$$\langle y\overline{v'c'}\rangle = \langle c\rangle K_y \tag{4a}$$

and

$$\langle z\overline{w'c'}\rangle = \langle c\rangle K_z, \tag{4b}$$

the correlations are closely identified with the turbulent diffusivity, and we obtain

$$\frac{d}{dt}\sigma_y^2 = 2K_y, \tag{5a}$$

$$\frac{d}{dt}\sigma_z^2 = 2K_z, \tag{5b}$$

$$\frac{d}{dt}K_y = \overline{v'^2} - A\frac{q}{\Lambda}K_y, \tag{5c}$$

$$\frac{d}{dt}K_z = \overline{w'^2} - A\frac{q}{\Lambda}K_z + \frac{g}{T_0}G_z, \tag{5d}$$

and

$$\frac{d}{dt}G_z = \overline{w'\theta'} - 2bs\frac{q}{\Lambda}G_z - \frac{\partial\bar{\theta}}{\partial z}K_z, \tag{5e}$$

where $G_z = \langle z\overline{c'\theta'}\rangle/\langle c\rangle$. In this form, the second-order closure model is seen to provide a dynamic equation for the diffusivity in terms of the velocity and temperature fluctuation correlations.

This brief discussion shows that a practical dispersion scheme for application in a Gaussian plume model can be derived from the second-order closure conservation equations. The inputs required for the scheme are the velocity and temperature fluctuation correlation profiles, as well as the turbulence length scale Λ. Discrete values are determined from an interpolation of the profiles at the vertical location of the plume centroid. Before discussing the modifications needed for the prediction of relative dispersion, however, we shall generalize the basic model to allow the description of anisotropic conditions.

Under many circumstances, and especially when buoyancy effects are significant, the vertical structure of the turbulence can be different from that in the horizontal. Vertical motions may be preferentially constrained by stable stratification or by the presence of the ground surface, and the description of such conditions requires separate length scales, Λ_y and Λ_z, for the horizontal and vertical, respectively. For atmospheric applications, the constraints virtually always apply to the vertical scale, so we shall assume $\Lambda_y \geq \Lambda_z$ throughout the following discussion. In conjunction with the directional scale specification, we must define a corresponding turbulence energy q^2. The horizontal component includes all the energy since it includes the larger

horizontal length scale, but the vertical component should only include eddies on the scale Λ_z, which may be smaller than Λ_y. We therefore define

$$q_y^2 = \overline{u'^2} + \overline{v'^2} + \overline{w'^2} \tag{6a}$$

and

$$q_z^2 = \sigma_u^2(\Lambda_z) + \sigma_v^2(\Lambda_z) + \overline{w'^2}, \tag{6b}$$

where $\sigma_u^2(\Lambda_z)$ represents the amount of the $\overline{u'^2}$ variance on scales smaller than or equal to Λ_z. This depends on the spectral shape, and we now proceed to a discussion of the appropriate representation.

3. Relative dispersion model

We need to distinguish between the meandering motions and the mixing eddies in the spectrum of velocity fluctuations, and this is accomplished through specification of the turbulence spectrum in terms of the length scales Λ_y and Λ_z. These scales will generally be functions of altitude and will be prescribed along with the turbulence profiles. The turbulent energy spectrum is considered to peak around the integral scale, with an inertial range cascade toward the small-scale dissipation range. Several analytic approximations for the complete turbulent energy spectrum have been suggested in the past, but we use a very simple representation that is consistent with the Kolmogorov $k^{-5/3}$ inertial range behavior. The turbulent energy contained in the spectrum for wavelengths shorter than l is defined by the power-law relation

$$\sigma_v^2(l) = \begin{cases} \overline{v'^2}\left(\dfrac{l}{\Lambda_y}\right)^{2/3}, & l \le \Lambda_y \\ \overline{v'^2}, & l \ge \Lambda_y. \end{cases} \tag{7}$$

A similar expression determines the vertical velocity variance σ_w^2, with $\overline{w'^2}$ and Λ_z in place of $\overline{v'^2}$ and Λ_y. This allows the turbulent velocity variance to be specified as a function of length scale and allows the portion of the spectrum responsible for plume mixing to be determined since we shall relate the scale l to the local plume size.

The essence of the relative dispersion model is an evolution equation for the spatial spreads in terms of the plume-scale mixing rates. This is obtained by using the local plume scale l and the plume-scale turbulence σ_v in the closure equations (5a)–(5e) in place of the overall scale Λ_y and the total variance $\overline{v'^2}$. Thus, for the horizontal diffusion, we obtain

$$\frac{d}{dt}\sigma_{yi}^2 = 2K_{yi} \tag{8a}$$

and

$$\frac{d}{dt}K_{yi} = \sigma_v^2(l_y) - A\frac{q_{yi}(l_y)}{l_y}K_{yi}, \tag{8b}$$

where the subscript i denotes the instantaneous value and q_{yi}^2 represents the velocity variance at the instantaneous horizontal plume scale.

The vertical dispersion equations are obtained in a very similar fashion, except for the further requirement that the heat flux correlation be specified as a function of local plume scale. The heat flux acts to enhance the vertical dispersion rate under convectively unstable conditions, but it is not appropriate to use the full correlation for instantaneous dispersion since a large part of the flux is carried by the large eddies and therefore contributes to the vertical plume meander. The inertial range theory of turbulent cospectra (Lumley 1967; Wyngaard and Coté 1972) predicts a $k^{-7/3}$ dependence for the heat flux—that is, a more rapid decay than that of the variance spectrum. This is consistent with the observation that the smaller-scale turbulence is more nearly isotropic, so the cross correlations become negligible for the smaller length scales. A simplified power-law behavior, similar to (7), for the heat flux contribution from length scales smaller than l is therefore given by

$$c_{w\theta}(l) = \begin{cases} \overline{w'\theta'}\left(\dfrac{l}{\Lambda_z}\right)^{4/3}, & l \le \Lambda_z \\ \overline{w'\theta'}, & l \ge \Lambda_z, \end{cases} \tag{9}$$

so that the spectrum falls much more rapidly than the velocity variances. The vertical dispersion equations then become

$$\frac{d}{dt}\sigma_{zi}^2 = 2K_{zi}, \tag{10a}$$

$$\frac{d}{dt}K_{zi} = \sigma_w^2(l_z) - A\frac{q_{zi}}{l_z}K_{zi} + \frac{g}{T_0}G_{zi}, \tag{10b}$$

and

$$\frac{d}{dt}G_{zi} = c_{w\theta}(l_z) - 2bs\frac{q_{zi}}{l_z}G_{zi} - \frac{\partial\bar{\theta}}{\partial z}K_{zi}, \tag{10c}$$

where the plume-scale energies are defined as

$$q_{yi}^2 = \sigma_u^2(l_y) + \sigma_v^2(l_y) + \sigma_w^2(l_y) \tag{11a}$$

and

$$q_{zi}^2 = \sigma_u^2(l_z) + \sigma_v^2(l_z) + \sigma_w^2(l_z). \tag{11b}$$

It only remains to determine the instantaneous length scales l_y and l_z, which we take to be proportional to the instantaneous plume spread; that is,

$$l_y = \min(\alpha_1\sigma_{yi}, \Lambda_y) \tag{12a}$$

and

$$l_z = \min(\alpha_1\sigma_{zi}, \Lambda_z), \tag{12b}$$

where α_1 is an empirical constant, which must be determined from experimental data. We compare the cur-

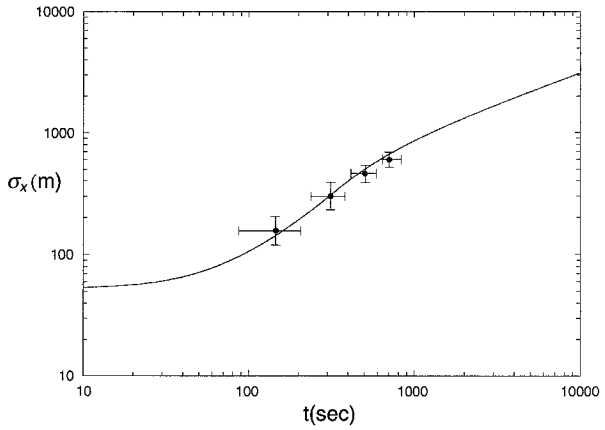

FIG. 1. Instantaneous spread comparison between the second-order closure dispersion model and the data of Weil et al. (1993).

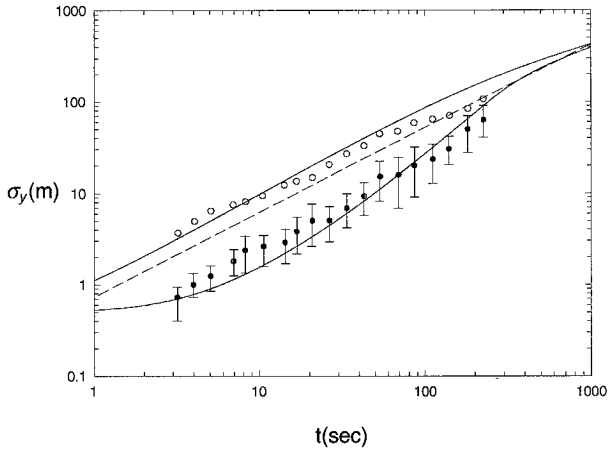

FIG. 2. Lateral spread comparison between the second-order closure dispersion model and the data of Mikkelsen et al. (1987). Solid circles are the instantaneous experimental data, and open circles are ensemble measurements. The closure model predictions are shown as solid lines, and the PGT stability C prediction is dashed.

rent model with experimental data on instantaneous dispersion in section 5, where it is shown that $\alpha_1 = 1.25$ gives reasonably good agreement with a number of observational datasets.

4. Effect of time averaging

The effects of finite sample time are accounted for by generalizing the spectral partition to account for the averaging period. As the plume sampling time is increased, it is clear that larger-scale turbulent motions will contribute to the measured plume size. If we can estimate the magnitude of the largest scale that contributes to the time-average dispersion, then we can replace the scale definition in (12) and simply use the dispersion model given in section 3.

Since a fixed sampler provides an Eulerian average, we derive the effective length scale using the mean wind speed. We also include a turbulent velocity scale, so that the length is well defined for light wind or calm conditions. Our simplified representation is given as

$$l_y = \min[\max(\Lambda_{\text{av}}, \alpha_1\sigma_{yi}), \Lambda_y] \tag{13a}$$

and

$$l_z = \min[\max(\Lambda_{\text{av}}, \alpha_1\sigma_{zi}), \Lambda_z], \tag{13b}$$

where Λ_{av} is defined as

$$\Lambda_{\text{av}} = \alpha_2 T_{\text{av}}(U^2 + q^2)^{1/2} \tag{14}$$

and T_{av} is the averaging time period.

The model (13a) and (13b) provides a continuous transition from the relative dispersion result for instantaneous sampling ($T_{\text{av}} = 0$) up to the ensemble average result for large T_{av}. The selection of the parameter α_2 must be based on experimental observations and is discussed in the next section.

5. Comparison with field data

a. Instantaneous dispersion

We first compare the second-order closure dispersion model described in section 3 with available experimental data on relative dispersion—that is, instantaneous sampling. The value for α_1 was selected to give an overall optimum agreement with data, and the ''best'' value, $\alpha_1 = 1.25$, is used in all the comparisons shown below. The optimum value for individual experiments varied between 1.0 and 1.5. The first data comparison uses the recent ice crystal experiment results of Weil et al. (1993). A vertical sheet of ice crystals was formed within a natural cloud by seeding with dry-ice pellets from an aircraft, and the spread (in the direction normal to the vertical sheet) of the ice crystal cloud was then measured from the aircraft, along with relevant turbulence statistics. There is significant scatter in the measured instantaneous cloud spread, and there is also significant uncertainty in the initial source size. Weil et al. (1993) presented averaged results for the dimensionless cloud spread from an ensemble of about 25 releases, and the data are compared with the closure model prediction in Fig. 1. We have used an initial source size of 53 m, which corresponds to the larger of the source sizes considered by Weil et al. (1993), and the data have been made dimensional using the observed average values $\overline{v'^2} = 3.6\ \text{m}^2\ \text{s}^{-2}$ and $\varepsilon = 0.013\ \text{m}^2\ \text{s}^{-3}$. We assume isotropic conditions to determine the other velocity variances, and the turbulence length scales are obtained from the dissipation rate (see Lewellen 1977) as

$$\Lambda_y = \Lambda_z = \frac{bq^3}{\varepsilon}. \tag{15}$$

This implies that $\Lambda_y = 341$ m for the Weil et al. (1993) data. Figure 1 shows that the second-order closure mod-

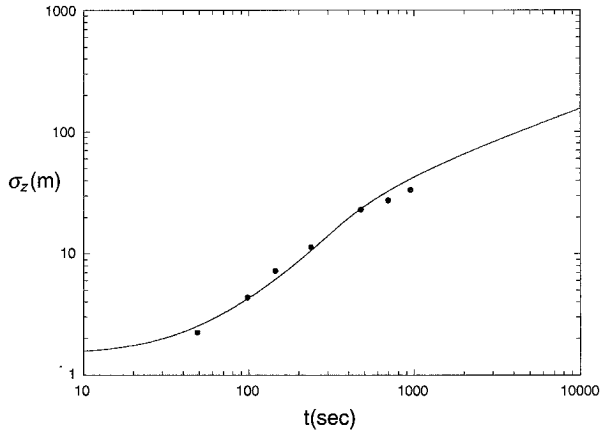

FIG. 3. Instantaneous vertical spread comparison between the second-order closure dispersion model and the data of Högström (1964).

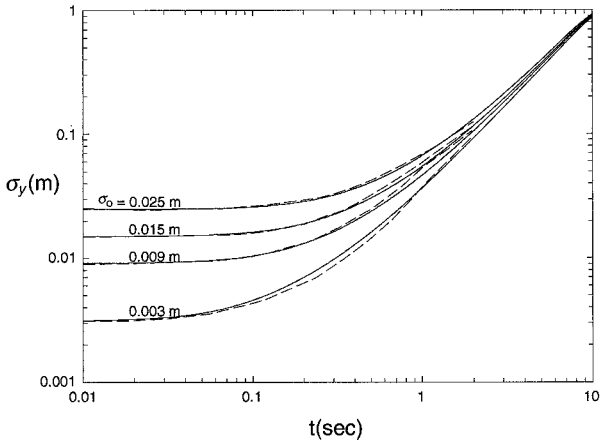

FIG. 4. Instantaneous lateral spread comparison between the second-order closure dispersion model and the model predictions of Fackrell and Robins (1982).

el provides reasonably good agreement with the data, although the data limitations and uncertainties preclude a detailed assessment.

Figure 2 shows the closure model comparison with the data of Mikkelsen et al. (1987), where both instantaneous and ensemble average lateral spread were measured. The experimental data are based on 22 photographic images of a surface-released smoke plume. The lateral turbulent velocity variance $\overline{v'^2}$ was measured as 0.98 m^2 s^{-2}, and the Lagrangian integral timescale is given as 100 s based on the measured Eulerian spectrum. The mean velocity at the plume height was 4.72 m s^{-1}. We again assume isotropic conditions for simplicity since the other turbulence components were not reported, although we note that this assumption is not strictly valid in the atmospheric surface layer. The length scale is derived from the Lagrangian timescale, which corresponds to Λ/Aq in the closure model, and the vertical and horizontal scales are assumed to be equal at 130 m. The initial source size is taken to be 0.5 m, corresponding to the larger value tested by Mikkelsen et al. (1987); the other value of 0.25 m gives marginally worse agreement with the data using the present closure model. The results are not sensitive to the assumption of isotropy since we use the observed value of the Lagrangian timescale to determine the length scale. A test calculation using $\Lambda_z = 6.5$ m, as appropriate for a plume at $z = 10$ m, and reducing the vertical velocity variance in accordance with the $-5/3$ law gave almost identical results to the isotropic calculation.

The lower curves in Fig. 2 show the instantaneous lateral spread prediction, which generally lies within the experimental error bounds. In addition, the figure shows the ensemble spread prediction as the upper line, which also compares well with the observations. The standard empirical Pasquill–Gifford–Turner (PGT) estimate for stability category C is shown as a dashed line in the figure and indicates that this prediction lies between the two extremes of the time averaging, although it is clearly closer to the ensemble average value.

Figure 3 compares the closure model prediction of vertical spread with the neutral relative dispersion data of Högström (1964), as described by Sawford (1982). The release was made at 50 m, and there is considerable uncertainty with regard to the turbulence conditions. We follow Sawford in determining the effective length scale from the late-time dispersion measurements. We use a turbulence intensity of 0.1, as suggested by Sawford, and again assume isotropic conditions. Thus, $\overline{u'^2} = \overline{v'^2} = \overline{w'^2} = 0.01U^2$, and the length scales Λ_y and Λ_z were taken to be 16 m. A source size of 1 m was used in the calculation since this is the midrange value considered by Sawford. The turbulence specifications enforce agreement with the data at late time, but the model does predict the proper early time growth of the plume. Note that the horizontal scale in the plot has been arbitrarily transformed into a time using an assumed mean wind speed of 1 m s^{-1}.

Fackrell and Robins (1982) used the Smith and Hay (1961) theory in conjunction with wind tunnel turbulence measurements to predict the instantaneous plume spread for a range of source sizes. These predictions were used to estimate the concentration fluctuation variance, using the meandering plume theory of Gifford (1959), and were compared with laboratory measurements, providing an indirect experimental verification for the spread predictions. Figure 4 shows the closure model lateral spread predictions for several source sizes compared with the Fackrell and Robins (1982) results for an elevated source. The closure model uses the observed turbulence values and length scales at the source height. The integral length scale was experimentally determined from the turbulent energy spectrum, and this can be related to the dissipation rate in the inertial range. The closure model relations were then used to determine Λ_y and Λ_z, which were assumed to be equal in this case.

The closure model agrees very well with the more sophisticated spectral analysis for the range of source sizes.

b. Time-average dispersion

Data on the direct effect of finite time averaging are scarce, but the commonly used PGT stability curves for short-range dispersion from surface releases are based on an averaging time of about 10 min, and therefore they provide a comparison for finite averaging time. The PGT classification system requires a self-similar solution to the diffusion equation, so that the plume spread is a function of downstream distance and stability class only. This is possible if the turbulent velocity scales are proportional to the transport speed and the turbulent length scales are only dependent on the vertical height. The standard surface-layer representation fulfills most of these conditions since the turbulence and mean wind speed are generally specified in terms of u_* and dimensionless height z/L, where L is the Monin–Obukhov length. The shear-driven component of the turbulence in the surface layer can be modeled (Townsend 1976) as

$$\overline{v_s'^2} = 2.5u_*^2 \tag{16a}$$

and

$$\overline{w_s'^2} = 1.5u_*^2, \tag{16b}$$

and we assume both horizontal and vertical length scales to be proportional to z; that is,

$$\Lambda_{ys} = \Lambda_{zs} = 0.65z. \tag{17}$$

The behavior of the horizontal scale is probably more complicated than (17), but we expect convective motions to dominate near the surface under unstable conditions and therefore use the simplified representation here.

The buoyancy-driven turbulence component is modeled using the convective scaling results of Deardorff (1970), which depend on the mixed-layer depth z_i, in addition to the Monin–Obukhov length. The horizontal velocity fluctuations are driven by the large eddies in the convective boundary layer and therefore do not scale with surface-layer variables. The buoyancy-driven turbulence correlations are modeled as

$$\overline{v_b'^2} = 0.325u_*^2\left(\frac{z_i}{-kL}\right)^{2/3} \tag{18a}$$

and

$$\overline{w_b'^2} = 1.15u_*^2\left(\frac{z_i}{-kL}\right)^{2/3}, \tag{18b}$$

where $k = 0.4$ is the von Kármán constant. The horizontal length scale is taken to be $\Lambda_{yb} = 0.3z_i$, and the vertical scale is the same as that for the shear component. We note that the buoyancy component requires knowledge of the mixed-layer depth, and we shall assume a fixed value of 1000 m for the comparisons below. Additionally, we assume Monin–Obukov lengths of -5, -12.5, -50, and -1000 m for PGT stability classes A, B, C, and D, respectively. The contributions from the shear and buoyancy components are scaled independently using (7), (13), and (14), and then combined by simple summation for use in the dispersion model equations.

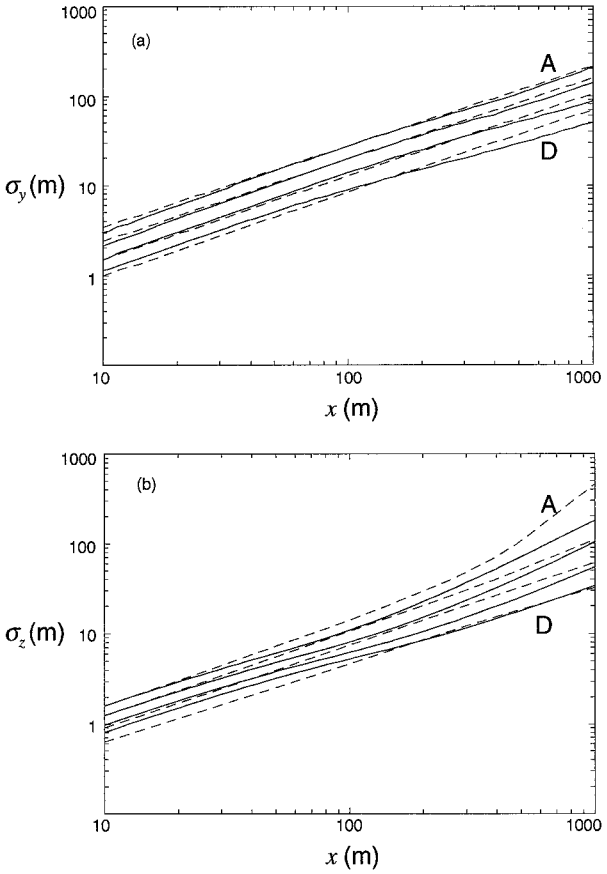

FIG. 5. Time-averaged spread comparison between the second-order closure dispersion model (solid) and the PGT correlations (dashed) of Stern et al. (1984) for stability classes A, B, C, and D. (a) Horizontal spread and (b) vertical spread.

With the above specifications for the turbulence, we can compute an almost self-similar solution for the vertical dispersion using the closure model, but the horizontal dispersion is more complicated. If we use a release at $z_{\text{rel}} = 5$ m with a surface roughness length of 3 cm and a wind speed of 5 m s^{-1} at $z = 10$ m, then a value of 0.02 for α_2 gives the best fit with the accepted PGT curves, but we emphasize that the results depend significantly on the wind speed. The model equations are integrated using the specified turbulence profiles and the height used in the integration is the larger of z_{rel} and σ_z. The closure model predictions for horizontal and vertical plume spread are shown in Fig. 5, and stable conditions are omitted since the horizontal turbulence generation mechanisms in a stable stratification are

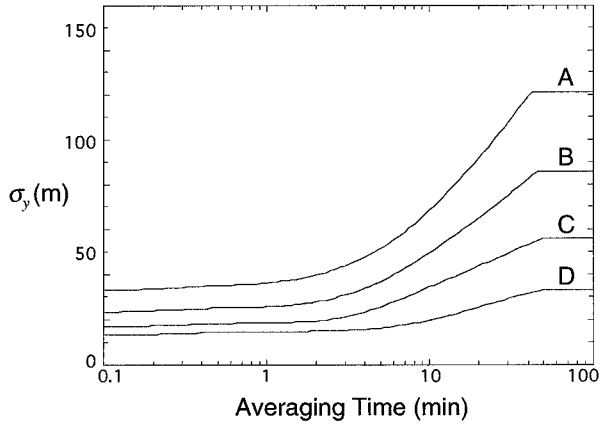

FIG. 6. Effect of time average on the second-order closure dispersion prediction for lateral spread at $x = 300$ m for PGT stability classes A, B, C, and D.

poorly understood. The closure model is in reasonable agreement with the generally accepted dispersion curves for surface-layer dispersion, although we note the dependence on wind speed and the associated uncertainty in the value of α_2.

The explicit effect of averaging time on the PGT dispersion results is illustrated in Fig. 6, which shows lateral spread at $x = 300$ m for the range of stability classes. The large-scale horizontal motions under convective conditions produce a strong dependence on averaging time since the source size is much smaller than the eddy size. As conditions become more neutral and more of the turbulent energy is contained in the surface-layer scales, the variation with averaging time is reduced. The discontinuity in the slope of the curves at the upper transition is due to the simplified representation of the spectrum in (7), which abruptly limits the velocity variance when the averaging scale reaches the turbulence scale. A smoother variation would be obtained from a more continuous description of the spectrum.

6. Summary

The effect of finite averaging time on the measured concentration of a contaminant can be important in assessing a number of effects from atmospheric pollutants, including plume visibility, flammability, toxicity, and chemical reaction rates. Averaging time affects the dispersion rate because the turbulent motions occur on a wide range of timescales and are not all sampled in a short-duration average. A proper prediction of the concentration level in a dispersing plume must therefore explicitly account for the averaging time in the turbulent diffusion calculation.

A simplified dispersion model based on a second-order turbulence closure scheme to account for averaging time effects on the dispersion rate has been presented. The model uses the Gaussian plume framework to provide a prediction of the lateral and vertical spread and extends the earlier work of Sykes et al. (1986) to account for finite averaging time. The reduced spread rate for short averaging times is modeled using a very simple representation of the turbulence spectrum to restrict the turbulent energy available for dispersion.

Eckmann (1994) has presented a model for the effect of time averaging, but a direct comparison is difficult since his nondimensionalization involves a spectral definition of the length scale k_0^{-1}, which must be related to our turbulence scale Λ. If we use numbers from the Borris Field Experiment data of Mikkelsen et al. (1987), Eckmann gives $k_0^{-1} = 278$ m, as compared to our estimated value of 130 m for Λ in section 3. The upper transition to the ensemble dispersion value occurs at $\alpha_2 UT_{av} \approx \Lambda$ from (13) and (14), which corresponds to a dimensionless averaging time of about 25 in Eckmann's notation and is reasonably consistent with his Fig. 4. We note, however, that the plume spread in our model occurs more rapidly as the upper transition is approached, and we therefore predict an effective transition to the ensemble value at a longer averaging time than Eckmann. A better representation of the spectrum would give a smoother transition to the ensemble spread.

The simple closure model presented above shows good agreement with experimental data from instantaneous and ensemble dispersion studies, but data for finite averaging time are lacking. The transition from instantaneous to ensemble or long time-average dispersion is not clearly delineated in existing experimental data and represents a source of uncertainty in the model evaluation. The simplified description of the turbulent energy spectrum in the current model may prove inadequate as more detailed measurements of plume spread as a function of averaging time become available. The closure framework is sufficiently general, however, that a more complex spectral description can easily be implemented as future experiments provide further information on the phenomenon.

Acknowledgments. This work was supported by the Electric Power Research Institute, with Pradeep Saxena as Program Manager.

REFERENCES

Batchelor, G. K., 1950: The application of the similarity theory of turbulence to atmospheric diffusion. *Quart. J. Roy. Meteor. Soc.*, **76,** 133–146.

Brier, G. W., 1950: The statistical theory of turbulence and the problem of diffusion in the atmosphere. *J. Meteor.*, **7,** 283–290.

Deardorff, J. W., 1970: Convective velocity and temperature scales for the unstable planetary boundary layer and for Rayleigh convection. *J. Atmos. Sci.*, **27,** 1211–1213.

Eckman, R. M., 1994: Influence of the sampling time on the kinematics of turbulent diffusion from a continuous source. *J. Fluid Mech.*, **270,** 349–375.

Fackrell, J. E., and A. G. Robins, 1982: The effects of source size

on concentration fluctuations in plumes. *Bound.-Layer Meteor.*, **22,** 335–350.
Georgopoulos, P. G., and J. H. Seinfeld, 1988: Estimation of relative dispersion parameters from atmospheric spectra. *Atmos. Environ.*, **22,** 31–41.
Gifford, F. A., 1959: Statistical properties of a fluctuating plume dispersal model. *Advances in Geophysics*, Vol. 6. Academic Press, 117–137.
Högström, U., 1964: An experimental study on atmospheric diffusion. *Tellus*, **16,** 205–251.
Lewellen, W. S., 1977: Use of invariant modeling. *Handbook of Turbulence*, W. Frost and T. H. Moulden, Eds., Plenum Press, 237–280.
Lumley, J. L., 1967: Theoretical aspects of research on turbulence in stratified flows. *Proc. Int. Colloquium Atmospheric Turbulence and Radio Wave Propagation*, Nauka, Moscow, 105–110.
Mikkelsen, T., S. E. Larsen, and H. L. Pécseli, 1987: Diffusion of Gaussian puffs. *Quart. J. Roy. Meteor. Soc.*, **113,** 81–105.
Sawford, B. L., 1982: Comparison of some different approximations in the statistical theory of relative dispersion. *Quart. J. Roy. Meteor. Soc.*, **108,** 191–206.
Slade, D. H., Ed., 1968: *Meteorology and Atomic Energy*. U.S. Atomic Energy Commission, Office of Information Services, 445 pp.
Smith, F. B., and J. S. Hay, 1961: The expansion of clusters of particles in the atmosphere. *Quart. J. Roy. Meteor. Soc.*, **87,** 82–101.
Stern, A. C., R. W. Boubel, D. B. Turner, and D. L. Fox, 1984: *Fundamentals of Air Pollution*. 2d ed. Academic Press, 544 pp.
Sykes, R. I., W. S. Lewellen, and S. F. Parker, 1986: A Gaussian plume model of atmospheric dispersion based on second-order closure. *J. Climate Appl. Meteor.*, **25,** 322–331.
Townsend, A. A., 1976: *The Structure of Turbulent Shear Flow*. Cambridge University Press, 438 pp.
Weil, J. C., R. P. Lawson, and A. R. Rodi, 1993: Relative dispersion of ice crystals in seeded cumuli. *J. Appl. Meteor.*, **32,** 1055–1073.
Wyngaard, J. C., and O. R. Coté, 1972: Cospectral similarity in the atmospheric surface layer. *Quart. J. Roy. Meteor. Soc.*, **98,** 590–603.